Single vs Dual ion UV–crosslinked gel polymer electrolytes for Li-O_2 batteries

*Marta Alvarez Tirado [a, b], Laurent Castro [b, *], Gregorio Guzmán-González [a], Luca Porcarelli [a,c], David Mecerreyes [a,d, *]*

[a] POLYMAT University of the Basque Country UPV/EHU, Avenida Tolosa 72, Donostia-San Sebastian 2008, Spain

[b] Toyota Motor Europe Research & Development 1, Advanced Material Research, Battery & Fuel Cell, Hoge Wei 33 B, B-1930 Zaventem, Belgium

[c] ARC Centre of Excellence for Electromaterials Science and Institute for Frontier Materials, Deakin University, Melbourne, Australia

[d] Ikerbasque, Basque Foundation for Science, E-48011, Bilbao, Spain.

AUTHOR INFORMATION

Corresponding Author

*e-mail: david.mecerreyes@ehu.es, Laurent.Castro@toyota-europe.com

ABSTRACT. Lithium-O_2 batteries represent one of the most appealing candidates for battery electric vehicles (BEV) due to its remarkable theoretical high energy density, similar to fossil fuels. Solid polymer electrolytes represent a plausible solution to tackle some of the challenges associated to conventional liquid-based Li-O_2 batteries, including safety concerns. Herein, cross-linked robust gel polymer electrolytes (GPE) based on poly(ethylene glycol) dimethacrylate (PEGDM) and tetraethylene glycol dimethyl ether (TEGDME) as plasticizer are prepared by rapid UV-photopolymerization. Both types of robust GPEs presented high ionic conductivity at room temperature ($1.6 \cdot 10^{-4}$ S·cm^{-1} and $1.4 \cdot 10^{-3}$ S·cm^{-1} for single ion or dual ion, respectively). Both types of GPEs, single ion and dual ion lithium conductors, have been compared for the first time on Li-O_2 cells. First, their performance was investigated in symmetrical Li|Li cells. In this case, the dual-ion GPE showed an outstanding behavior where the overpotential was <0.2 V vs Li^0/Li^+ for more than 40 hours at a current density as highs as ±1 mA·cm^{-2}. On the other hand, in full Li-O_2 configuration, the single ion GPE cell showed superior discharge capacity, up to 2.38 mAh·cm^{-2}. A dynamic discharge characterization technique is proposed here as a method for evaluating the polarization effect in electrolytes during discharge in an easy, quantifiable and reproducible manner.

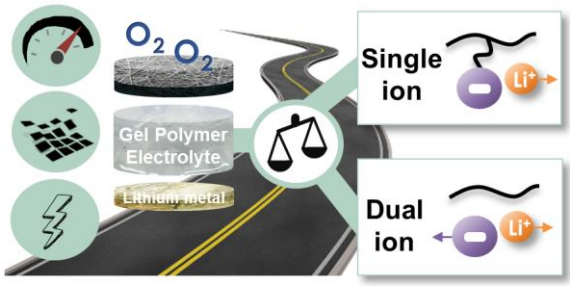

KEYWORDS

Solid electrolytes; Li-O_2 batteries; Gel polymer electrolytes; Single ion; Dynamic discharge

1. INTRODUCTION

Lithium-ion batteries, whilst very popular for many applications such as portable electronics, may be limited for others such as battery electric vehicles (BEV) in which a higher energy density is desired[1]. In that sense, technologies such as rechargeable lithium-air/Li-O_2 batteries are attractive candidates due to their theoretical specific energy density (11,000 Wh/kg for Li_2O_2 formation), which is comparable to gasoline (13,000 Wh/kg)[2–4]. However, the full deployment of this technology has not yet been possible due to a number of unsolved challenges, such as the liquid electrolyte degradation in the presence of oxo-radicals[5–7]. The electrolyte plays an essential role on Li-O_2 batteries as it determines the electrochemical reactions. Aprotic liquid electrolyte cells, also called "non-aqueous", are the most popular due to their highest theoretical capacity[8]. Common aprotic solvents are organic carbonates (e.g. propylene carbonate, PC); ethers (e.g. dimethoxyethane, DME); others such as dimethyl sulfoxide (DMSO)[7] or ionic liquids[9,10]. Among all, tetraethylene glycol dimethyl ether (TEGDME) is the most used liquid electrolyte due its low volatility, wide electrochemical window (beyond 4.5 V versus Li^0/Li^+) good solubility of metal alkali salts and relatively low cost[11–15]. However, its liquid nature prompts some drawbacks related to safety issues such as the potential leaking of the toxic and flammable organic electrolyte in the cell[16].

Beyond conventional liquid electrolytes, solid polymer electrolytes (SPEs) represent a plausible solution to tackle these challenges[17,18]. However, their ionic conductivity is still several orders of magnitude lower than the liquid cells (10^{-5}-10^{-6} S·cm^{-1} for SPE vs 10^{-2}-10^{-3} S·cm^{-1} for liquid)[19]. A compromising solution could be the so-called gel polymer

electrolytes (GPEs), in which a solvent (often named plasticizer) is trapped within the polymer network. This configuration shows an intermediate ionic conductivity (~10^{-3} to 10^{-4} S·cm^{-1})[20]. Latest studies on polymer-based GPE electrolytes for Li-O_2 applications include complex hybrid composite systems, in which lithium active (e.g. $Li_{7-3x}Al_xLa_3Zr_2O_{12}$) or passive (e.g. Al_2O_3) inorganic fillers are also added[11]. In general, the ionic conductivities reported in these systems[21–27] are ≤10^{-3} S·cm^{-1} and lithium platting/stripping behaviors in symmetrical cells are limited to 0.1–0.2 mA·cm^{-2}, with the exception of a recently published hybrid PVDF-HFP/PMMA/SiO_2 system[24] that was cycled at 0.5 mA·cm^{-2}. Reported performance on Li-O_2 cells were promising. For example, Yu and co-workers constructed a novel ultra-dry polymer electrolyte based on P(VDF-HFP) that achieved ~2600 mAh·g^{-1} at 0.4 mA·cm^{-2} [27]. In another approach, Kim and co-workers managed to remarkably increase the discharge capacity of their GPE based on PAN from 894 mAh·g^{-1} to 4059 mAh·g^{-1}, thanks to tetrachloro-1,4-benzoquinone (tCl-pBQ) redox mediator[21].

All the studies shown above developed systems based on different lithium salts (e.g. $LiCF_3SO_3$, LiTFSI, $LiClO_4$, $LiNO_3$, etc) in combination with a polymer matrix and a plasticizer. Alternatively to these salt-systems, in which both the lithium ion and the counter anion are moving in the cell (dual ion systems), single ion conducting polymer electrolytes have drawn great attention the last years due to its good performance when lithium metal is used in the negative electrode[28–33]. Within single ion polymer electrolytes, attaching the anion covalently to the polymer chain restricts the anion mobility to one of the lithium cation. Although lithium single ion conductors are very popular in lithium metal batteries with different inorganic cathode materials, to the best of our knowledge, they have not been

investigated yet in Li-O_2 applications. Only a single ion GPE based on lithiated perfluorinated sulfonic ionomer (i.e. Nafion™) swollen in DMSO, named as PFSA-Li, has been considered by Yang et al.[34,35]. The PFSA-Li soft membrane showed an ionic conductivity of $6.4 \cdot 10^{-4}$ S·cm^{-1} at RT and a promising cycling stability at 1 A·g^{-1} of 55 cycles. Performance on symmetrical cells was limited to 60 hours at 0.25 mA·cm^{-2} with overpotentials <0.1 V vs Li^0/Li^+. The aim of our article is to compare for the first time single ion and dual ion conducting GPEs, and their liquid counterparts, and to evaluate their performance in Li-O_2 cells. Herein, we present two comparable solid gel polymer electrolytes (GPE) using the most successful electrolyte (TEGDME) as plasticizer for their potential use as solid electrolytes for Li-O_2 batteries. For this purpose, a new electrochemical methodology based on dynamic discharge was assessed as a new way to weigh the polarization effect during Li-O_2 discharge.

2. RESULTS AND DISCUSSION

As shown in Scheme 1, Single ion GPEs were prepared by UV-co-polymerization of poly(ethylene glycol) dimethacrylate (PEGDM) and lithium 1-[3-(methacryloyloxy)-propylsulfonyl]-1-(trifluoromethylsulfonyl)imide (LiMTFSI) in the presence of TEGDME as a plasticizer and using 2-Hydroxy-2-methylpropiophene (DAROCUR) as a radical photoinitiator. Dual ion GPEs were elaborated in a similar manner, in which PEGDM was UV-polymerised in the presence of a liquid electrolyte composed by lithium bis(trifluoromethanesulfonyl)imide (LiTFSI) dissolved in TEGDME. UV-photopolymerization was selected due to the simplicity and rapidness of the approach and its previous success on many types of batteries[31,36]. In both cases, self-standing, flexible and visually transparent membranes (Figure 1a) could be obtained until a plasticizer content of

80%wt approximately. Samples with concentrations of TEGDME higher than >80 %wt. were too soft and difficult to handle. According to the Fourier Transform Infrared Spectroscopy (FTIR) spectra, monomer conversions higher than ≥95% were reached by the disappearance of the 1635 cm^{-1} band, which is associated to the carbon double bond of methacrylates[37] (Figure S1).

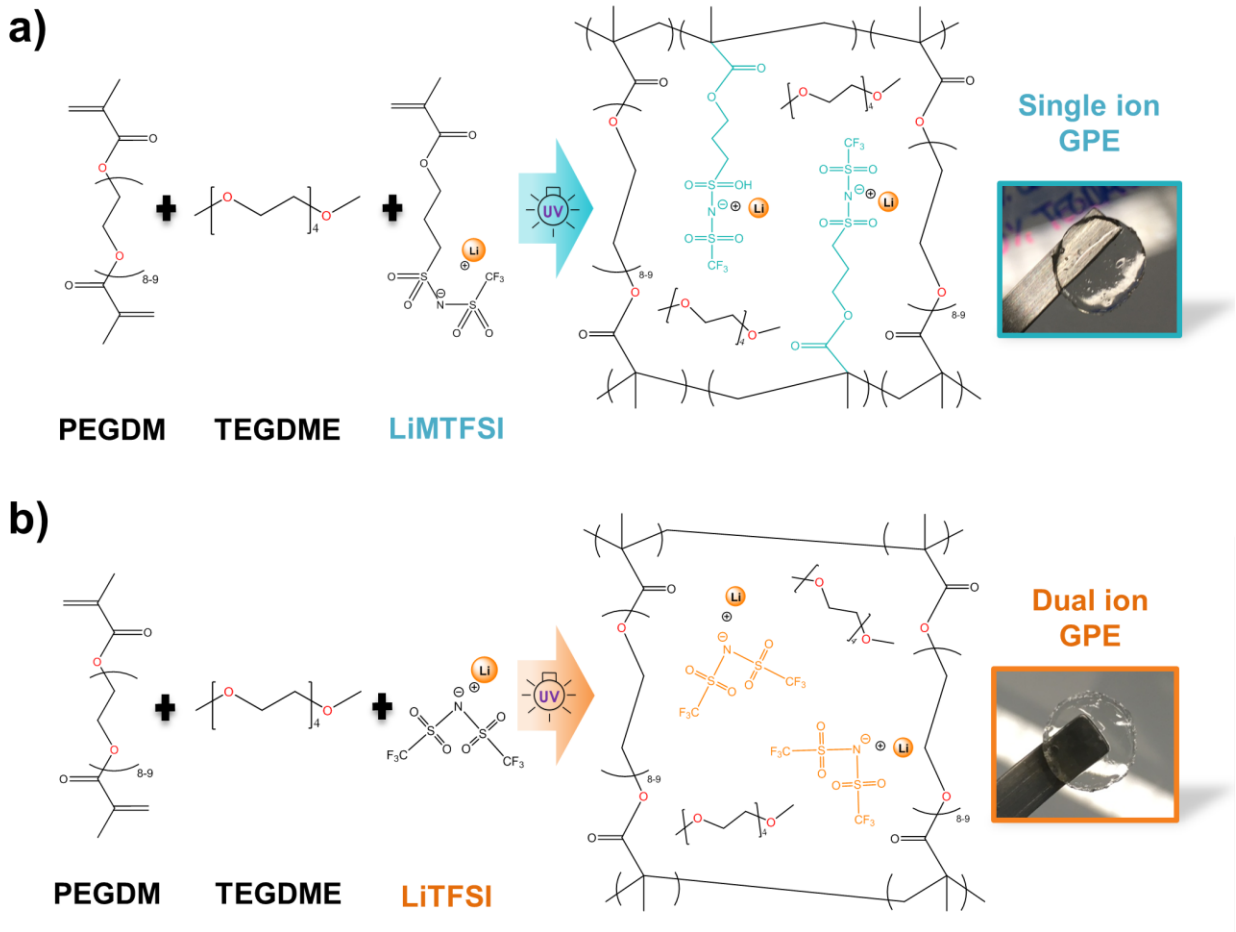

Scheme 1. Schematic representation of the preparation of both a) Single ion and b) Dual ion gel polymer electrolytes (GPEs) by UV–photopolymerization.

To down select the best single-ion GPE formulations, the ionic conductivity (σ) of GPEs with different compositions was evaluated at 25 °C (battery operating temperature). For the

design of the single ion GPEs, the concentration of the LiMTFSI monomer in the formulation was varied from 10 to 30 %wt., keeping fixed the cross-linker concentration at 10 %wt. As shown in Figure 1b, the inclusion of higher concentrations of single-ion lithium monomer did not imply a higher σ. In fact, the more lithium monomer, the more polymer matrix and therefore less plasticizer in the GPE; limiting the movement of ions. Thus, there was a tradeoff between plasticizer and polymer ratio. In this case, the sample 20 %wt. LiMTFSI : 70% wt. TEGDME : 10 %wt. PEGDM, showed the highest conductivity value of $1.64 \cdot 10^{-4}$ $S \cdot cm^{-1}$ and was selected for further testing. From now on, this formulation is named in the article as "**Single ion GPE**". Ionic conductivity data measured for all single ion GPEs by electrochemical impedance spectroscopy (EIS) in the full temperature range between 25 and 85 °C data is shown in Figure S2. As indicated before, a dual ion conductive GPE membrane was designed incorporating the same molar ratio of lithium. Hence, the selected **"Dual ion GPE"** formulation showing the highest ionic conductivity was 90 %wt. (0.84M LiTFSI in TEGDME) : 10 %wt. PEGDM. Figure 1c shows the ionic conductivity of these two membranes measured at different temperatures. The σ of the equivalent liquid electrolyte (0.84M LiTFSI in TEGDME) was also assessed for reference. The Dual ion GPE achieved $1.44 \cdot 10^{-3}$ $S \cdot cm^{-1}$ at 25°C, showing a value very close to the liquid electrolyte of similar composition $2.88 \cdot 10^{-3}$ $S \cdot cm^{-1}$. As expected, the σ of the Single ion GPE was lower than the Dual ion one, in where a slightly higher content of plasticizer was present and we were capturing the conductivity of both highly mobile [$TFSI^-$] and [Li^+] ions. The proportion of the conductivity that is carried by the lithium cations can be quantified[38], the so-called lithium transference number (t^+_{Li}). The method proposed by Evans-Vincent-Bruce[38,39] was used to measure the t^+_{Li} of both Single ion and Dual ion GPEs. Results of EIS and polarizations tests at 25°C are shown in

Figure S3 (Supporting Information). The transference number value of the Single ion GPE was found to be 0.83 ± 0.01; while the Dual ion GPE reached 0.57 ± 0.02. In single ion GPEs, the plasticizer (e.g. TEGDME) can form solvated complexes with the lithium ions, allowing their free movement and achieving t^{+}_{Li} close to unity[30,35]. For dual ion GPE electrolytes, t^{+}_{Li} values are usually lower (around 0.5-0.6)[40,41] due to the high mobility of the sulphonamide anion compared to the bulky solvated lithium shell[42]. Hence, these results are comparable to ones found in literature (Table S2, Supporting Information).

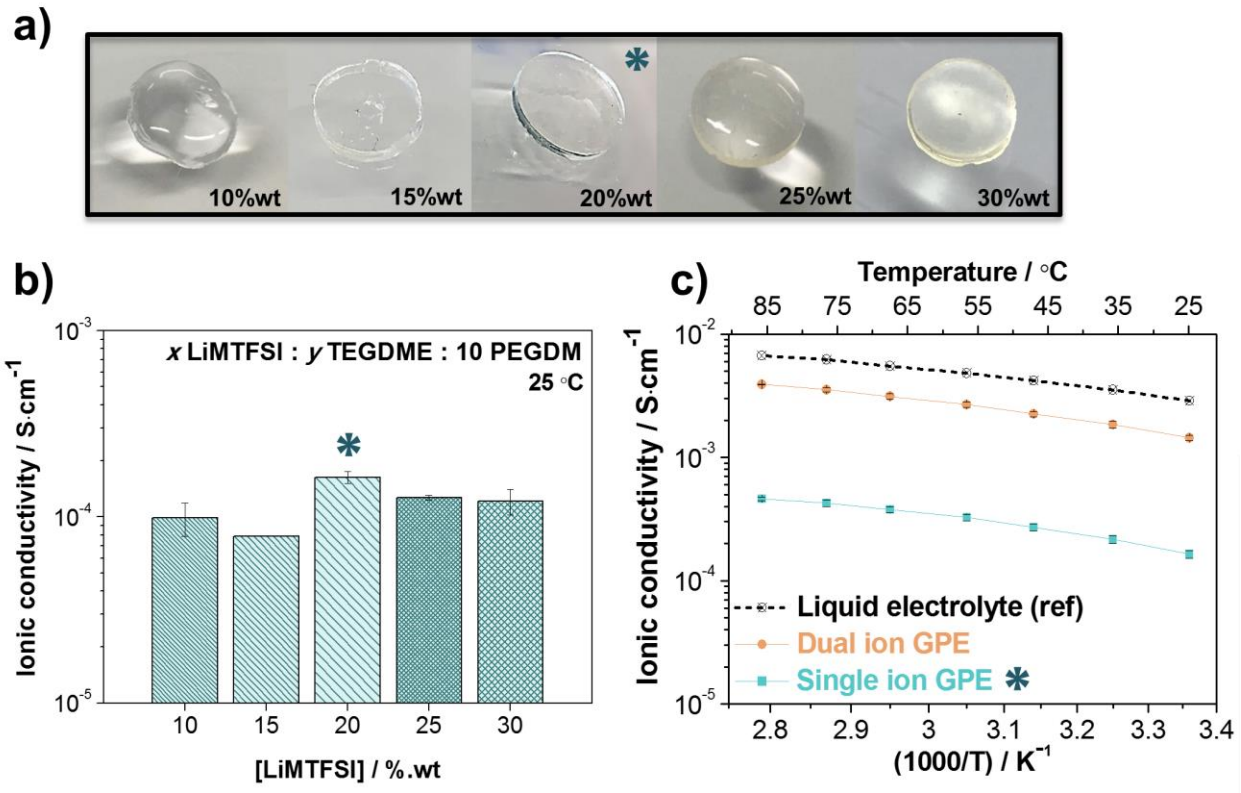

Figure 1. a) Images of the single ion membranes containing increasing amount of lithium conductive monomer (LiMTFSI) in wt%., b) Ionic conductivity values of single ion conducting GPEs having 10, 15, 20, 25 and 30 %wt. of LiMTFSI monomer in their formulation at 25°C and, c) Ionic conductivity vs temperature of selected Single ion (*) and Dual ion GPE compared to the analogue liquid electrolyte.

All these samples were further tested from a mechanical and thermal perspective. The thermal stability was assessed by thermal gravimetrical analysis (TGA) under inert atmosphere (N_2) as shown on Figure 2a. In all cases, the samples exhibited a two-step degradation process and curves were slightly shifted at different temperatures, depending on the composition. The initial degradation, between 150 – 200 ºC, was attributed to the initial loss of TEGDME. This was more significant in the samples with larger amount of plasticizer (10 : 80 : 10 and Dual ion GPE, which had 80 and 90 %wt. of liquid electrolyte, respectively), achieving loses of up to 60% of their weight at 200 ºC. The second degradation, initiated at around 250 ºC, was greatly attributed to the degradation of the polymeric matrix[30]. Therefore, the TGA curves of the single ion GPEs with higher concentrations of polymer were shifted to the right. In this second range, the final evaporation of the remaining TEGDME was also considered due to its low volatility (bp 275 ºC). The curve of the dual ion behaved slightly differently on the second step due to the presence of the TFSI Lithium salt. Dynamic mechanical thermal analysis (DMTA) was also assessed, Figure 2b. As expected, the storage modulus of the samples increased with the polymer concentration achieving a maximum of $2.53 \cdot 10^5$ Pa for the 30 : 60 : 10 membrane. Thus, this sample was stiffer but also more brittle (high cross-linking). The modulus of the Single ion GPE* was one order of magnitude higher than the Dual ion GPE ($3.45 \cdot 10^4$ and $2.24 \cdot 10^3$ Pa, respectively) remaining steady from 0 to 100 ºC. To conclude this section, the optimized UV-crosslinked GPEs showed excellent ionic conductivity values, good thermal and mechanical stability, which makes them interesting materials for battery applications in temperature ranges bellow 100 ºC.

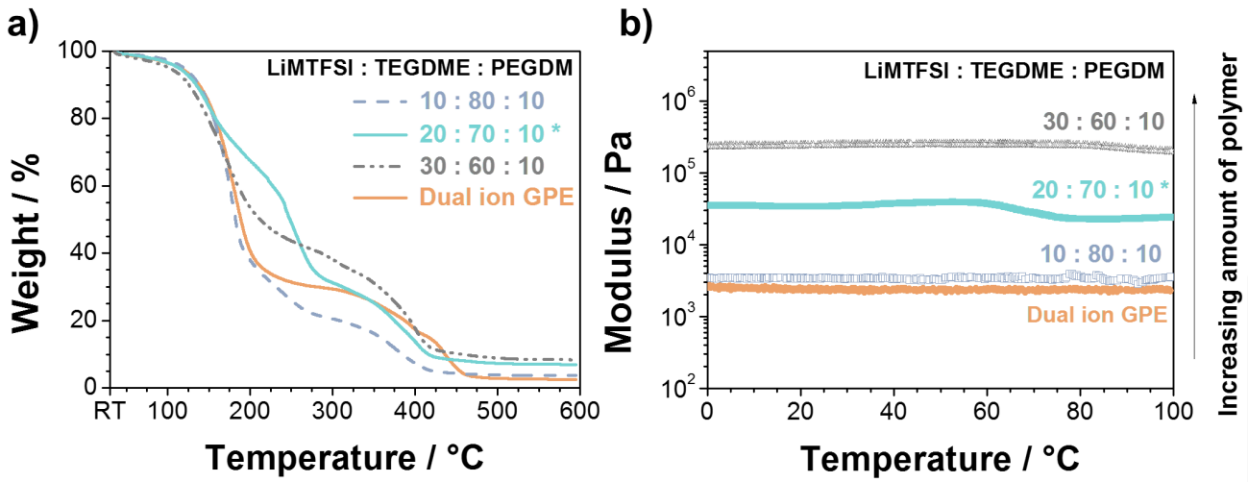

Figure 2. Characterization techniques applied to the solid Dual ion GPE and three different single-ion membranes having increasing concentrations of LiMTFSI conducting monomer (10, 20 and 30 %wt.): a) TGA analysis under nitrogen atmosphere at 10 ºC/min and b) DMTA analysis at compression from 0 to 100 ºC.

Next, symmetrical lithium cells were assembled to evaluate the electrochemical behavior of the solid electrolytes against lithium metal under different current densities (Figure S4). Firstly, the samples were exposed to ±0.01, ±0.1, ±0.2, ±0.5, ±0.8, ±1 and ±2 mA·cm^{-2} current rates for one hour / rate, also called "ramp test". Two cycles were completed for a total of 84 hours as shown on Figure 3a. The data was then handled for both cycles, to directly compare the absolute potential achieved at each current density with a 10 V cut-off. As shown on the curves of the first cycle (Figure 3b), the Dual ion GPE showed much lower overpotentials than the Single ion GPE, exceptionally being 0.3 V vs Li^0/Li^+ at 1 mA·cm^{-2} and only 1.5 V vs Li^0/Li^+ at 2 mA·cm^{-2}. On the other hand, the overpotentials achieved on the second cycle increased significantly in the case of the Single ion GPE (~3 times the initial value, at 0.2 or 0.5 mA·cm^{-2}). This tendency remarkably differed on the Dual ion GPE, in which the

overpotential remained steady at 0.3 V vs Li^0/Li^+ when 1 $mA \cdot cm^{-2}$ was applied. Due to this promising behavior, the Dual ion GPE was then further exposed to lithium plating/striping cycles of increasing rates from ±0.2, ±0.5, ±0.8 to ±1 $mA \cdot cm^{-2}$ with a cut-off potential of 0.5 V and half-cycle time of one hour. As shown on Figure 3c, the sample was able to cycle for 40 hours at high current (1 $mAh \cdot cm^{-2}$) below 0.2 V vs Li^0/Li^+. Furthermore, the overpotential was still below 0.4 V after 55 hours of cycling. Liquid cells were also tested in this configuration, as shown in Figure S5. All in all, polymer GPEs electrolytes behaved as good as their liquid counterparts and the Dual ion GPE, which had a highest ionic conductivity value, showed much better performance in lithium symmetrical cells. This result was initially surprising as single ion electrolytes are expected to show lower overpotentials during lithium plating/stripping. There is a study from Lee J.T. research group[43], in which they compared a single and dual ion electrolyte in lithium symmetrical cells. Their conclusion was that their single ion electrolyte behaved better than the dual ion only at lower currents. At higher currents, their dual ion sample exceeded the single ion. They explained this behaviour via the higher inherent impedance of the single ion system, especially noticeable at higher currents. This probably explain the results of this article since the current rates (up to 2 $mA \cdot cm^{-2}$) are much higher than the ones usually reported in literature in symmetrical lithium cells (0.1 – 0.5 $mA \cdot cm^{-2}$)[20,24,30,41].

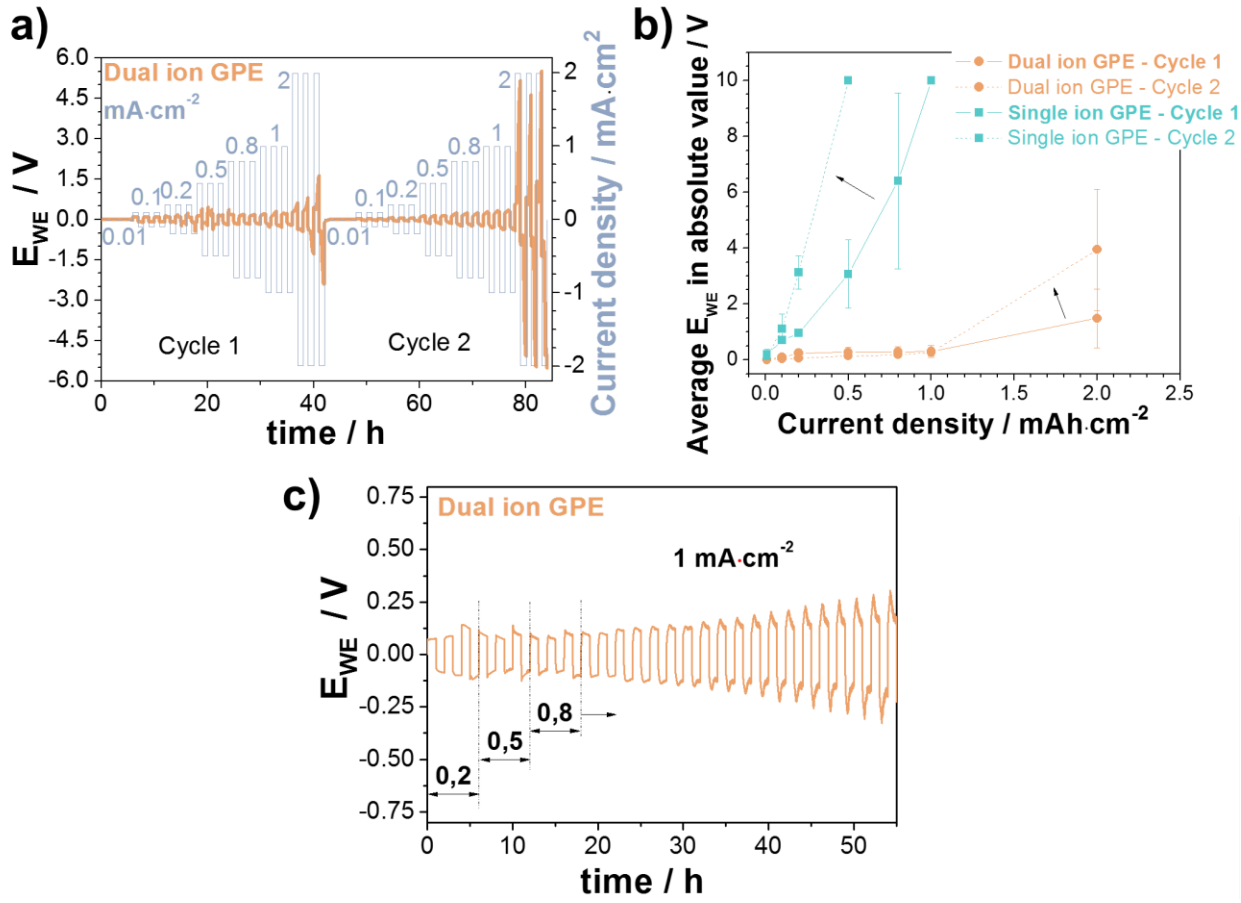

Figure 3. Tests undertaken on lithium symmetric cells: a) Ramp test divided in two cycles with increasing current densities from 0.01 to 2 mA·cm^{-2}. Potential against time data for Li | Dual ion GPE | Li cell, b) Absolute potential against current density of Single ion and Dual ion GPEs. Data extracted from ramp test, and c) lithium plating/striping cycles on Dual ion GPE, applying up to 1 mA·cm^{-2}.

To further evaluate and compare the performance of the single and dual ion GPE membranes, they were tested on Swagelok Li-O_2 cells as shown on Figure 4b (look for further details on electrode materials in the Supporting Information). Together with the solid electrolytes GPEs, cells using liquid electrolytes were prepared and tested for comparison. The equivalent dual/single liquid electrolytes were based on TEGDME dissolutions

concentrated at 0.84 M LiTFSI or LiMTFSI, respectively. These cells were firstly discharged at a galvanostatic current of –5 μA·cm^{-2} (Figure 4a) until the potential reached 2 V at 25 °C. When the negative current was applied, the samples first suddenly experimented an Ohmic drop (*iR*), reaching quickly a plateau at around 2.78 V, which corresponds to the practical potential of the spontaneous electrochemical reaction $2Li + O_2 + 2e^- \rightarrow Li_2O_2$ (lower than the theoretical one (2.96V vs Li^0/Li^+)) due to overpotentials)[3,5] followed by a sharped decrease to 2.0 V vs. Li^0/Li^+ at the end of the discharging[44]. As shown in the graph, the Single ion GPE achieved the highest absolute capacity for this first discharge, being 1.5 times higher than the Dual ion GPE (2.38 and 1.56 mAh·cm^{-2}, respectively). Most likely, this is due to the fact that only Li^+ ions are moving on the Single ion membrane, which allows a more homogeneous and ordered mass transfer of cations to the positive electrode, especially, for low current densities (i.e. –5 μA·cm^{-2}). Similar conclusions were achieved in other studies done on lithium metal batteries[43]. Interestingly, the GPE solid electrolytes achieved much higher capacity than their liquids counterparts: 1.7 times higher in the case of Single ion samples and 1.25 times for the Dual ion ones. Considering an average carbon loading of 0.72 mg·cm^{-2} in the positive electrode, the relative capacity was as high as 3306 and 2190 mAh·g^{-1} for the Single and Dual ion GPEs, respectively. In order to provide insights into the rechargeability of the developed electrolytes, discharge/charge cycles at ±50 μA·cm^{-2} for both Single ion and Dual ion Li-O_2 cells are shown in Figure S6 (Supplementary Information).

Furthermore, samples were discharged following a dynamic approach, in which increasing negative currents were applied to the sample (Figure 4c-f). Each current density was applied for 15 minutes and immediately increased and re-applied for another 15 minutes, in a similar

way to GITT test (Galvanostatic Intermittent Titration Technique). This increasing current approach was done until the potential of the cell faded below 2 V and OCV was then applied (Figure 4c). Interestingly, the potential of the cell increased back to equilibrium values during OCV. After sufficient time and when $dE_{WE} / dt \sim 0$, the cell was dynamically discharged again (named as second loop). The potential increased back again to equilibrium and the cell was discharged again (named as third loop). This innovative process was repeated until the equilibrium potential of the cell at OCV was below 2 V vs Li^0/Li^+ (Figure 4d), allowing a gradual discharge of the cell. The number of repetitions of this process (named as loops) may differed between samples because of the maximum currents achieved at each loop, as shown in Figure 4f. As an example, the Single ion GPE discharged after 52 loops, the Dual ion GPE after 36 loops, and their equivalent liquid cells after 45 and 43 loops, respectively.

The potentials at equilibrium after a single dynamic discharge (one loop) ($E2_{eq}$ in Figure 4d), were proportional to the polarization effect of all the Li cations accumulated at the positive electrode that were unable to react with the oxo- radicals due to the short times applied at each rate (15 minutes), the increasing current densities (diffusional limitation at higher rates) and/or the inability to find a free active site on the carbon electrode (i.e. pseudo-capacitive contribution of the battery). During OCV, these unreacted ions re-arranged and, consequently, the potential first suddenly increased to a value proportional to the Ohmic drop (*iR*) and then, it slowly increased (ions diffusion phenomena due to concentration gradients after applying current) until equilibrium, i.e. $dE_{WE} / dt \approx 0$.

Relevant information can be extracted from the raw data of the multiple dynamic discharge. In each loop, the sample is able to withstand a determined maximum current density. The higher this current is, the better; especially if it is maintained over different loops. This information is plotted in Figure S7 (single loop) and Figure 4f (multiple loops). In general, all samples behaved similarly, with the exception of the Dual ion GPE. The majority of them showed low variations on the maximum currents achieved across discharge (~flat curve), being the polymeric samples superior than their liquid counterparts. On the other hand, the Dual ion GPE exhibited remarkable high current densities, with a maximum of 350 $\mu A \cdot cm^{-2}$ and being above 175 $\mu A \cdot cm^{-2}$ when the cumulative capacity was already as high as 2.4 $mAh \cdot cm^{-2}$. This outstanding performance against high currents is in accordance with the results obtained on the symmetrical lithium cells.

Furthermore, the equilibrium polarization potentials can be plotted against their cumulative capacity (Figure 4e). The shape of the curves strongly reminds to the galvanostatic discharge curves, which is in accordance with the above explanation (gradual discharge of the cell). As observed, the highest cumulative capacity corresponds with the Dual ion GPE (3.46 $mAh \cdot cm^{-2}$ or 4824 $mAh \cdot g^{-1}$), followed by the Single ion GPE (2.86 $mAh \cdot cm^{-2}$ or 3984 $mAh \cdot g^{-1}$) and the equivalent liquid cells (2.44 and 1.97 $mAh \cdot cm^{-2}$ for the LiMTFSI and LiTFSI liquid electrolytes, respectively). Figuratively, these results seems to be in contradiction with the galvanostatic discharge ones (Figure 4a). However, as these equilibrium potentials were proportional to the polarization effect, it would be accurate to expect higher cumulative capacities for the Dual ion system than the Single ion one; in one hand due to the higher amount of mobile ions (Li^+ and $TFSI^-$) and, on the other hand, due to

the higher maximum currents that the Dual ion GPE was able to withstand and therefore, higher cumulative capacities were achieved. This effect was also observed in other studies[43], and could be related to the intrinsic impedance of the Single ion GPE, which was higher than the one of the Dual ion GPE. This mass transfer limitation, related to the impedance, is therefore more pronounced when higher currents are applied according to the Ohmic law and Nernst-Planck equation[45]. Otherwise, this polarization effect seemed to be higher on the polymeric systems than the liquid equivalents. This could be due to the theoretical higher diffusion of ions in the liquid systems and the better wettability of the electrolyte | electrode interface.

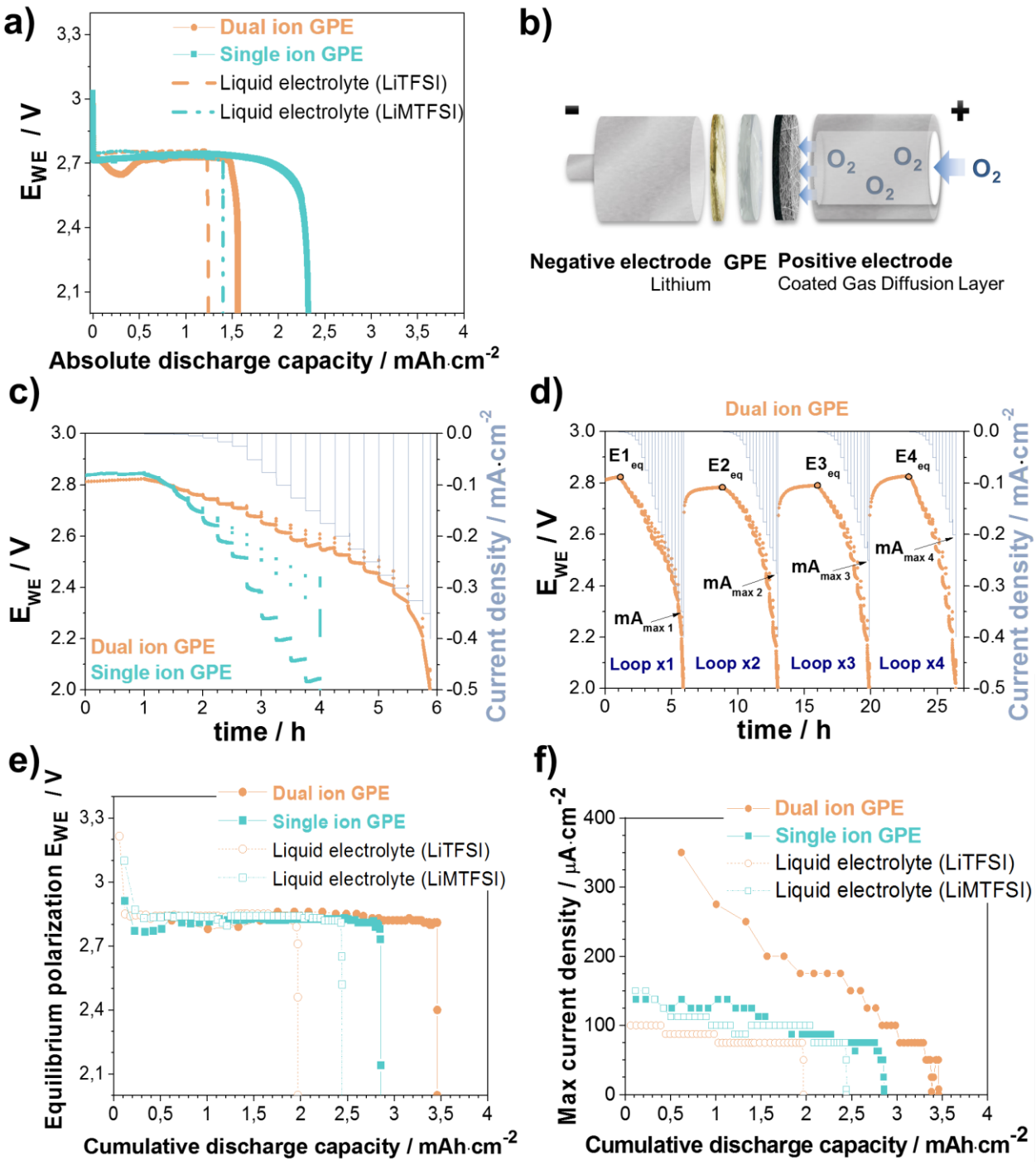

Figure 4. Tests carried out on Swagelok cells adopted to Li-O_2, including a new electrochemical characterisation method based on dynamic discharge. The electrolytes tested are Single and Dual ion GPEs as solid electrolytes, and their equivalent liquid electrolytes: a) plot of potential against absolute discharge capacity during galvanostatic

discharge at -5 μA·cm^{-2}, b) scheme of Swagelok Li-O_2 cell, c) plot of potential against time during the first loop of dynamic discharge for both Dual ion and Single ion GPEs electrolytes (raw data), d) innovative plot of potential against time during the first fourth loops of dynamic discharge using Dual ion GPE as a solid electrolyte (raw data), being the number of loops dependent to the type of electrolyte, e) plot of equilibrium polarization potentials against cumulative capacity during dynamic discharge, and f) maximum current densities stood by the electrolytes during dynamic discharge.

3. CONCLUSIONS

In conclusion, single ion gel polymer electrolytes based on TEGDME have been compared for the first time to its dual ion GPE counterparts as solid electrolytes for Li-O_2 batteries. These two new families of electrolytes were prepared in a simple manner by fast UV-photopolymerization. Gel polymer electrolytes showed a powerful combination of high ionic conductivity ($1.64 \cdot 10^{-4}$ S·cm^{-1} single ion < $1.44 \cdot 10^{-3}$ S·cm^{-1} dual ion at 25°C) mechanical strength ($3.45 \cdot 10^{4}$ single ion > $2.24 \cdot 10^{3}$ Pa dual ion) and good thermal stability (T_{onset} 150 °C similar in both cases). These properties make both GPEs feasible alternatives to liquid Li-O_2 cells. This study directly compares key features of two GPE systems by common characterization techniques and a new method to evaluate polarization effect during discharge. The Dual ion GPE showed a superior behaviour against high rates, even after long cycling in lithium symmetrical cells. On the other side, Single ion GPE showed excellent performance and higher capacities than the dual ion GPE in Li-O_2 cells. Interestingly, both solid GPEs behaved as good as or in a superior manner than their liquid electrolyte counterparts, settling a step forward to solid and safer Li-O_2 systems. The results showed in

this work could help in the design of future all-in-one electrolyte materials for multilayer Lithium Oxygen cells, in which a combination of different chemical structures might be needed.

4. EXPERIMENTAL SECTION

Experimental details can be found in the Supporting Information.

ASSOCIATED CONTENT

Supporting Information.

Experimental section, FTIR spectra on GPEs, ionic conductivities, chronoamperometry and EIS curves, lithium transference number reported in literature, scheme of lithium symmetric cell configuration, plots of potential profiles for Single and Dual ion GPEs compared with their liquid counterparts in symmetrical cells, plots of absolute capacity against potential during galvanostatic discharge/charge, and plot of potential profiles against current densities during dynamic discharge for Swagelok Li-O2 cells using single ion GPE, dual ion GPE and their equivalent liquid electrolyte cells.

Author information

*E-mail 1: david.mecerreyes@ehu.es Group Website http:// www.polymat.eu/en/groups/innovative-polymers-group. Group Twitter account: @DavidMecerreyes.

*E-mail 2: Laurent.Castro@toyota-europe.com

Notes: The authors declare no competing financial interest.

ACKNOWLEDGMENT

This work was supported by the European Commission´s funded Marie Skłodowska-Curie project POLYTE-EID (Project No. 765828). L.P. has received funding from the European Commission Horizon 2020 research and innovation programme under the Marie

Skłodowska-Curie Grant Agreement No. 797295 (eJUMP). G.G-G. is grateful to "Secretaría de Estado de Ciencia, Tecnología e Innovación" from Ciudad de Mexico for the current postdoctoral fellowship (SECTEI/133/2019). The manuscript was written through contributions of all authors that have given approval to the final version of the Letter.

REFERENCES

(1) Rahman, M. A.; Wang, X.; Wen, C. A Review of High Energy Density Lithium-Air Battery Technology. *J. Appl. Electrochem.* **2014**, *44* (1), 5–22.

(2) Song, M. K.; Park, S.; Alamgir, F. M.; Cho, J.; Liu, M. Nanostructured Electrodes for Lithium-Ion and Lithium-Air Batteries: The Latest Developments, Challenges, and Perspectives. *Mater. Sci. Eng. R Reports* **2011**, *72* (11), 203–252.

(3) Girishkumar, G.; McCloskey, B.; Luntz, A. C.; Swanson, S.; Wilcke, W. Lithium-Air Battery: Promise and Challenges. *J. Phys. Chem. Lett.* **2010**, *1* (14), 2193–2203.

(4) Sun, C. Recent Advances in Lithium-Air Batteries. *Adv. Mater. Lett.* **2018**, *9* (5), 336–344.

(5) Grande, L.; Paillard, E.; Hassoun, J.; Park, J. B.; Lee, Y. J.; Sun, Y. K.; Passerini, S.; Scrosati, B. The Lithium/Air Battery: Still an Emerging System or a Practical Reality? *Adv. Mater.* **2015**, *27* (5), 784–800.

(6) Lu, J.; Lau, K. C.; Sun, Y.-K.; Curtiss, L. A.; Amine, K. Review—Understanding and Mitigating Some of the Key Factors That Limit Non-Aqueous Lithium-Air Battery Performance. *J. Electrochem. Soc.* **2015**, *162* (14), A2439–A2446.

(7) Kwak, W.-J.; Rosy; Sharon, D.; Xia, C.; Kim, H.; Johnson, L. R.; Bruce, P. G.; Nazar, L. F.; Sun, Y.-K.; Frimer, A. A.; Noked, M.; Freunberger, S. A.; Aurbach, D. Lithium–Oxygen Batteries and Related Systems: Potential, Status, and Future. *Chem. Rev.* **2020**.

(8) Tan, P.; Jiang, H. R.; Zhu, X. B.; An, L.; Jung, C. Y.; Wu, M. C.; Shi, L.; Shyy, W.; Zhao, T. S. Advances and Challenges in Lithium-Air Batteries. *Appl. Energy* **2017**, *204*, 780–806.

(9) Mohzhukhina, N.; Tesio, A. Y.; Pozo, M. del; Calvo, E. J. Communication—Lithium Ion Concentration Effect in PYR 14 TFSI Ionic Liquid for Li-O 2 Battery Cathodes . *J. Electrochem. Soc.* **2017**, *164* (8), H5277–H5279.

(10) Ha, T. A.; Fdz De Anastro, A.; Ortiz-Vitoriano, N.; Fang, J.; MacFarlane, D. R.; Forsyth, M.; Mecerreyes, D.; Howlett, P. C.; Pozo-Gonzalo, C. High Coulombic Efficiency Na-O2 Batteries Enabled by a Bilayer Ionogel/Ionic Liquid. *J. Phys. Chem. Lett.* **2019**, *10* (22), 7050–7055.

(11) Li, B.; Liu, Y.; Zhang, X.; He, P.; Zhou, H. Hybrid Polymer Electrolyte for Li–O 2 Batteries. *Green Energy Environ.* **2019**, *4* (1), 3–19.

(12) Nasybulin, E.; Xu, W.; Engelhard, M. H.; Nie, Z.; Burton, S. D.; Cosimbescu, L.; Gross, M. E.; Zhang, J. G. Effects of Electrolyte Salts on the Performance of Li-O2 Batteries. *J. Phys. Chem. C* **2013**, *117* (6), 2635–2645.

(13) Wu, S.; Tang, J.; Li, F.; Liu, X.; Zhou, H. Low Charge Overpotentials in Lithium-Oxygen Batteries Based on Tetraglyme Electrolytes with a Limited Amount of Water. *Chem. Commun.* **2015**, *51* (94), 16860–16863.

(14) Zhao, Q.; Zhang, Y.; Sun, G.; Cong, L.; Sun, L.; Xie, H.; Liu, J. Binary Mixtures of Highly

Concentrated Tetraglyme and Hydrofluoroether as a Stable and Nonflammable Electrolyte for Li-O2 Batteries. *ACS Appl. Mater. Interfaces* **2018**, *10* (31), 26312–26319.

(15) Chamaani, A.; Safa, M.; Chawla, N.; El-Zahab, B. Composite Gel Polymer Electrolyte for Improved Cyclability in Lithium-Oxygen Batteries. *ACS Appl. Mater. Interfaces* **2017**, *9* (39), 33819–33826.

(16) Mauger; Julien; Paolella; Armand; Zaghib. Building Better Batteries in the Solid State: A Review. *Materials (Basel).* **2019**, *12* (23), 3892.

(17) Armand, M. The History of Polymer Electrolytes. *Solid State Ionics* **1994**, *69* (3), 309–319.

(18) Yi, J.; Guo, S.; He, P.; Zhou, H. Status and Prospects of Polymer Electrolytes for Solid-State Li–O 2 (Air) Batteries. *Energy Environ. Sci.* **2017**, *10* (4), 860–884.

(19) Elia, G. A.; Hassoun, J. A Polymer Lithium-Oxygen Battery. *Nat. Publ. Gr.* **2015**, *5*, 5:12307.

(20) Zou, X.; Lu, Q.; Zhong, Y.; Liao, K.; Zhou, W.; Shao, Z. Flexible, Flame-Resistant, and Dendrite-Impermeable Gel-Polymer Electrolyte for Li–O2/Air Batteries Workable Under Hurdle Conditions. *Small* **2018**, *14* (34), 1–10.

(21) Kim, Y. B.; Kim, I. T.; Song, M. J.; Shin, M. W. Synthesis of a Polyacrylonitrile/Tetrachloro-1,4-Benzoquinone Gel Polymer Electrolyte for High-Performance Li-Air Batteries. *J. Memb. Sci.* **2018**, *563* (March), 835–842.

(22) Pan, J.; Li, H.; Sun, H.; Zhang, Y.; Wang, L.; Liao, M.; Sun, X.; Peng, H. A Lithium–Air Battery Stably Working at High Temperature with High Rate Performance. *Small* **2018**, *14* (6), 1–6.

(23) Ren, M.; Zhang, J.; Zhang, C.; Stanford, M. G.; Chyan, Y.; Yao, Y.; Tour, J. M. Quasi-Solid-State Li-O2 Batteries with Laser-Induced Graphene Cathode Catalysts. *ACS Appl. Energy Mater.* **2020**, *3*, 1702–1709.

(24) Yang, T.; Shu, C.; Zheng, R.; Li, M.; Hou, Z.; Hei, P.; Zhang, Q.; Mei, D.; Long, J. Dendrite-Free Solid-State Li-O2 Batteries Enabled by Organic-Inorganic Interaction Reinforced Gel Polymer Electrolyte. *ACS Sustain. Chem. Eng.* **2019**, *7* (20), 17362–17371.

(25) Zhao, C.; Liang, J.; Zhao, Y.; Luo, J.; Sun, Q.; Liu, Y.; Lin, X.; Yang, X.; Huang, H.; Zhang, L.; Zhao, S.; Lu, S.; Sun, X. Engineering a "Nanonet"-Reinforced Polymer Electrolyte for Long-Life Li-O2 Batteries. *J. Mater. Chem. A* **2019**, *7* (43), 24947–24952.

(26) Balaish, M.; Leskes, M.; Ein-Eli, Y. Investigation of Rechargeable Poly(Ethylene Oxide)-Based Solid Lithium-Oxygen Batteries. *ACS Appl. Energy Mater.* **2018**, *1* (7), 3048–3056.

(27) Yu, W.; Xue, C.; Hu, B.; Xu, B.; Li, L.; Nan, C. W. Oxygen- and Dendrite-Resistant Ultra-Dry Polymer Electrolytes for Solid-State Li–O2 Batteries. *Energy Storage Mater.* **2020**, *27* (October 2019), 244–251.

(28) Phan, T. N. T.; Ferrand, A.; Ho, H. T.; Liénafa, L.; Rollet, M.; Maria, S.; Bouchet, R.; Gigmes, D. Vinyl Monomers Bearing a Sulfonyl(Trifluoromethane Sulfonyl) Imide Group: Synthesis and Polymerization Using Nitroxide-Mediated Polymerization. *Polym. Chem.*

2016, *7* (45), 6901–6910.

(29) Meabe, L.; Goujon, N.; Li, C.; Armand, M.; Forsyth, M. Single-Ion Conducting Poly (Ethylene Oxide Carbonate) as Solid Polymer Electrolyte for Lithium Batteries. *Batter. Supercaps* **2020**, *3*, 68–75.

(30) Porcarelli, L.; Shaplov, A. S.; Bella, F.; Nair, J. R.; Mecerreyes, D.; Gerbaldi, C. Single-Ion Conducting Polymer Electrolytes for Lithium Metal Polymer Batteries That Operate at Ambient Temperature. *ACS Energy Lett.* **2016**, *1* (4), 678–682.

(31) Sutton, P.; Airoldi, M.; Porcarelli, L.; Martínez, J. L. O.; Mugemana, C.; Bruns, N.; Mecerreyes, D.; Steiner, U.; Gunkel, I. Tuning the Properties of a UV - Polymerized , Cross - Linked Solid Polymer Electrolyte for Lithium Batteries. *Polymers (Basel).* **2020**, *12*, 595.

(32) Zhang, H.; Li, C.; Piszcz, M.; Coya, E.; Rojo, T.; Rodriguez-Martinez, L. M.; Armand, M.; Zhou, Z. Single Lithium-Ion Conducting Solid Polymer Electrolytes: Advances and Perspectives. *Chem. Soc. Rev.* **2017**, *46* (3), 797–815.

(33) Deng, K.; Zeng, Q.; Wang, D.; Liu, Z.; Qiu, Z.; Zhang, Y.; Xiao, M.; Meng, Y. Single-Ion Conducting Gel Polymer Electrolytes: Design, Preparation and Application. *J. Mater. Chem. A* **2020**, *8* (4), 1557–1577.

(34) Wu, C.; Liao, C.; Li, T.; Shi, Y.; Luo, J.; Li, L.; Yang, J. A Polymer Lithium-Oxygen Battery Based on Semi-Polymeric Conducting Ionomers as the Polymer Electrolyte. *J. Mater. Chem. A* **2016**, *4* (39), 15189–15196.

(35) Shi, Y.; Wu, C.; Li, L.; Yang, J. A Lithiated Perfluorinated Sulfonic Acid Polymer

Electrolyte for Lithium-Oxygen Batteries. *J. Electrochem. Soc.* **2017**, *164* (9), A2031–A2037.

(36) De Anastro, A. F.; Porcarelli, L.; Hilder, M.; Berlanga, C.; Galceran, M.; Howlett, P.; Forsyth, M.; Mecerreyes, D. UV-Cross-Linked Ionogels for All-Solid-State Rechargeable Sodium Batteries. *ACS Appl. Energy Mater.* **2019**, *2* (10), 6960–6966.

(37) Nyquist, R. A.; Fiedler, S.; Streck, R. Infrared Study of Vinyl Acetate , Methyl Acrylate and Methyl Methacrylate in Various Solvents. *Vib. Spectrosc.* **1994**, *6*, 285–291.

(38) Zugmann, S.; Fleischmann, M.; Amereller, M.; Gschwind, R. M.; Wiemhöfer, H. D.; Gores, H. J. Measurement of Transference Numbers for Lithium Ion Electrolytes via Four Different Methods, a Comparative Study. *Electrochim. Acta* **2011**, *56* (11), 3926–3933.

(39) Evans, J.; Vincent, C. A.; Bruce, P. G. Electrochemical Measurement of Transference Numbers in Polymer Electrolytes. *Polymer (Guildf).* **1987**, *28* (13), 2324–2328.

(40) Lv, Y.; Li, Z.; Yu, Y.; Yin, J.; Song, K.; Yang, B.; Yuan, L.; Hu, X. Copper/Cobalt-Doped LaMnO3 Perovskite Oxide as a Bifunctional Catalyst for Rechargeable Li-O2 Batteries. *J. Alloys Compd.* **2019**, *801*, 19–26.

(41) Yang, T.; Shu, C.; Zheng, R.; Hu, A.; Hou, Z.; Li, M.; Ran, Z.; Hei, P.; Long, J. Excellent Electrolyte-Electrode Interface Stability Enabled by Inhibition of Anion Mobility in Hybrid Gel Polymer Electrolyte Based Li-O2 Batteries. *J. Memb. Sci.* **2020**, *604* (October 2019), 118051.

(42) Fong, K. D.; Self, J.; Diederichsen, K. M.; Wood, B. M.; McCloskey, B. D.; Persson, K. A. Ion Transport and the True Transference Number in Nonaqueous Polyelectrolyte

Solutions for Lithium Ion Batteries. *ACS Cent. Sci.* **2019**, *5* (7), 1250–1260.

(43) Rohan, R.; Kuo, T. C.; Chen, M. W.; Lee, J. T. Nanofiber Single-Ion Conducting Electrolytes: An Approach for High-Performance Lithium Batteries at Ambient Temperature. *ChemElectroChem* **2017**, *4* (9), 2178–2183.

(44) Wang, Y.; Lai, N. C.; Lu, Y. R.; Zhou, Y.; Dong, C. L.; Lu, Y. C. A Solvent-Controlled Oxidation Mechanism of Li2O2 in Lithium-Oxygen Batteries. *Joule* **2018**, *2* (11), 2364–2380.

(45) Bard, Allen J.; Faulkner, L. R. . *ELECTROCHEMICAL METHODS - Fundamentals and Applications*, Second edi.; Harris, D. E. S., Ed.; JOHN WILEY & SONS, INC.: Austin, 2001; Vol. 2.